

# Defect Generation in Mono-layer Graphene in O<sub>2</sub>-PDA and FGA

W. J. Liu, K. Nagashio, T. Nishimura and A. Toriumi

Department of Materials Engineering, The University of Tokyo

7-3-1 Hongo, Bunkyo-ku, Tokyo, 113-8656, Japan

Phone: +81-3-5841-7161, E-mail: [liu@adam.t.u-tokyo.ac.jp](mailto:liu@adam.t.u-tokyo.ac.jp)

## Abstract

Either post deposition annealing (PDA) or forming gas annealing (FGA) is to improve the top-gate dielectric devices. However, it would degrade the graphene because of possible reactions of graphene. This paper discusses the defect generation in mono-layer graphene under both O<sub>2</sub>-PDA and FGA.

## 1. Introduction

Graphene has emerged as a promising material for various practical device applications. To make graphene applicable for practical devices and circuits, the top-gated graphene device is much more required, compared to back-gated devices. However, it is quite tough to form a high-quality or uniform top gate dielectric stack on graphene because of no dangling bonds on two-dimensional material. In addition, although the post-deposition O<sub>2</sub> annealing (O<sub>2</sub>-PDA) or forming gas annealing (FGA) is needed to achieve high quality dielectric films, in the meanwhile it may degrade graphene quality owing to a possible reaction between graphene and O<sub>2</sub> or H<sub>2</sub> molecules. Prior to the formation of top-gate dielectric, it is of significant importance to understand the characteristics of graphene without top-gate dielectric under such ambient annealing. The thermal treatment for conventional gate dielectrics usually needs around 600°C, which also restricts the PDA process for graphene. This paper reports how the defects are generated in mono-layer graphene (MLG) against O<sub>2</sub> and Ar/H<sub>2</sub> at elevated temperatures. Defects were estimated by microscopic Raman measurement and atomic force microscopy (AFM).

## 2. Experimental

MLG was transferred onto a 90-nm-thick SiO<sub>2</sub>/p<sup>+</sup>-Si substrate by the micromechanical cleavage of Kish graphite. Prior to graphene transfer, SiO<sub>2</sub>/Si substrates were annealing at 1000°C for 5 minutes in 100% O<sub>2</sub> flow. Graphene flakes were annealed in 100% O<sub>2</sub> or Ar/H<sub>2</sub> (5%), respectively, for 30 minutes as a function of annealing temperature in a home-made tube furnace. The number of graphene layers were detected by optical contrast and further verified by Raman spectra. Before and after annealing, Raman spectroscopy measurements of graphene layers were performed with  $\lambda = 488$  nm Ar laser (Horiba HR800) with a power of  $\sim 0.5$  mW at the sample position, which was set to prevent potential damage to graphene during the measurement. The laser spot size at focus and the resolution of the wavenumber were  $\sim 1$   $\mu$ m dia. and  $\sim 0.3$  cm<sup>-1</sup>, respectively.

## 3. Results and Discussion

Fig. 1 shows typical results of mono-layer graphene in the Raman measurement as a function of annealing temperature in O<sub>2</sub>. The D band peak obviously increases with the increase of annealing temperature. To improve the accuracy, the semi-log scales were used to estimate the D and G peak magnitude. Additionally, both G and 2D bands have a blue-shift after an O<sub>2</sub> annealing, which can be clearly seen in Fig. 1.

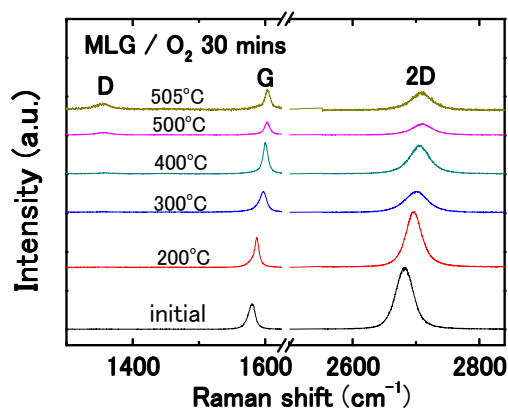


Fig.1 Typical Raman spectra of mono-layer graphene for several kinds of annealing temperature in O<sub>2</sub>.

The Raman intensity of D band over G band,  $I_D/I_G$ , as a function of temperature is summarized in Fig.2. It is obviously observed that two kinds of defect generation processes are overlapped in MLG. It appears a special corner-point of 400°C in defects generation process along the temperature, as denoted in Fig.2. Below the corner-point the defects generation in O<sub>2</sub> annealing is quite insensitive to the temperatures.

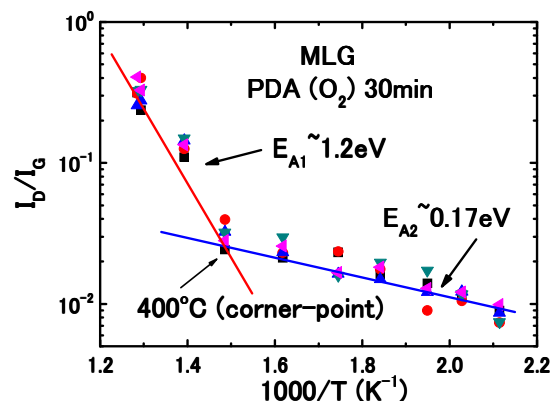


Fig.2  $I_D/I_G$  as a function of  $1/T$  in O<sub>2</sub> annealing. Two kinds of activation energies are clearly observed.

More interestingly, the defects generation is prominent above the corner-point. The results indicate that two independent activation processes are involved in the degradation process, which can be described as follows,

$$I_D/I_G = A_1 \exp\left(-\frac{E_{A1}}{k_B T}\right) + A_2 \exp\left(-\frac{E_{A2}}{k_B T}\right) \quad (1)$$

where  $A_1$ ,  $A_2$  are constants,  $E_{A1}$  and  $E_{A2}$  are activation energy ( $E_A$ ) above and below the corner-point, respectively. In case of MLG,  $E_{A1}$  and  $E_{A2}$  are estimated to be 1.2eV and 0.17eV, respectively, from the fitting.  $E_{A2}$  in the temperature range below the corner-point is negligibly small, possibly resulting from the thermal mismatch between graphene and SiO<sub>2</sub>/Si substrate. Above the corner-point  $E_A$  of 1.2eV should be much more concerned, which is corresponding to the oxygen effect in the annealing.

In the O<sub>2</sub>-PDA, the defect generation is dominated by the chemical reaction between graphene and O<sub>2</sub> at elevated temperatures, especially above the corner-point. As a matter of fact, the etching “pits” are detected after O<sub>2</sub> annealing as shown in Fig. 3 [1]. Therefore, it is quite natural that  $E_{A1}$  of 1.2eV should be related to the C-O bond breaking, very similar to the theoretical expectation of 1.5eV in graphene oxide [2]. This fact is quite suggestive of the G-O bond formation in O<sub>2</sub>-PDA.

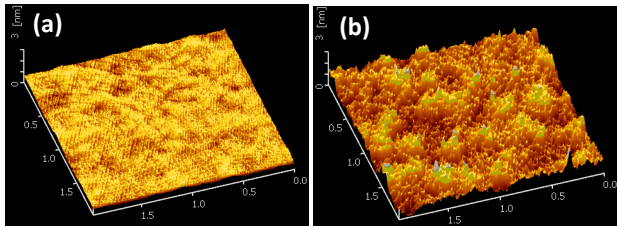


**Fig.3** 3-dimensional AFM image of MLG before (a) and after (b) an O<sub>2</sub> annealing at 500°C for 30 minutes. RMS is 0.1nm for the former and ~0.3nm for the latter, respectively.

Fig.4 shows temperature evolution of  $I_D/I_G$  of MLG in FGA for 30 minutes. Below 450°C,  $I_D/I_G$  is very small and almost keeps unchanged.  $E_A$  above 400°C in FGA is only 0.28eV, which is quite different from PDA in O<sub>2</sub>, in case  $E_{A1}$  is 1.2eV. It is interestingly pointed out that  $E_A$  (0.3eV)

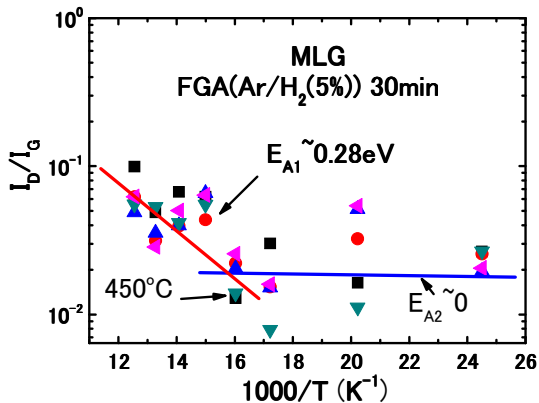


**Fig.4**  $I_D/I_G$  as a function of  $1/T$  in the Ar/H<sub>2</sub> (5%) annealing. Two regions are also observed.

in FGA above the corner-point is similar to  $E_{A2}$  (0.17) in O<sub>2</sub>-PDA below the corner-point, though whether the defects are also generated by thermal mismatch expansion in case of FGA or not obviously needs further investigations.

Indeed, we observed prominent differences in Raman spectra between O<sub>2</sub>-PDA and FGA treated graphene. The Raman spectra of MLG at 500°C for both O<sub>2</sub>-PDA and FGA are compred in Fig.5. It appears that D band is broadened and the “baseline” is also enhanced in FGA, marked by the red dash in Fig.5(a). Furthermore, though the G band near the center is still sharp, its tails seem to extend to some extent, as shown in Fig.5(a). This phenomenon is similar to that observed in disordered carbon[3] and CVD graphene heated in vacuum [4]. The band spectral broadenings indicates that a structure disorder occurs in MLG after FGA [4, 5], which may result from the heating effect and/or the small amount reactions between graphene and remaining H<sub>2</sub>, or O<sub>2</sub> and H<sub>2</sub>O underneath graphene. It is worth noting that the heating effect also exists, though the reaction between graphene and O<sub>2</sub> dominates the defect generation above the corner-point in case of O<sub>2</sub>-PDA.

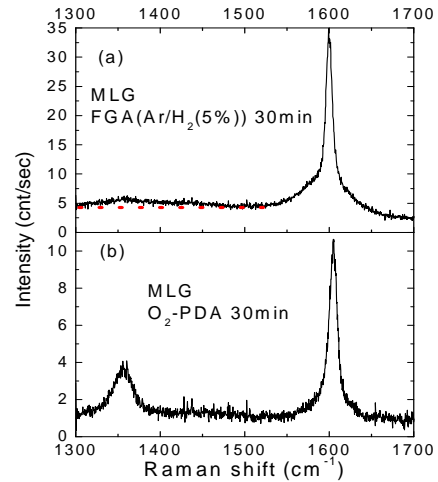


**Fig.5** Raman spectra of MLG at 500°C for both (a) FGA and (b) O<sub>2</sub>-PDA .

#### 4. Conclusions

The defect generation in MLG in both O<sub>2</sub>-PDA and FGA was investigated. Two kinds of activation energies are observed. Above the corner-point,  $E_A$  for O<sub>2</sub>-PDA is 1.2eV while ~0.3eV for FGA. The present results point out more importantly that the thermal treatment in O<sub>2</sub> even below 400°C for the top-gate graphene device integration may affect the graphene characteristics.

#### Acknowledgement

W. J. Liu is grateful to the Japan Society for the Promotion of Science (JSPS) for financial support. Kish graphite was provided from Covalent Materials Corporation.

#### References

- [1] L. Liu *et al.*, *Nano Lett.*, **8**, 1965 (2008). [2] R. Lahaye *et al.*, *PRB*, **79**, 125435 (2009). [3] A. C. Ferrari *et al.*, *PRB*, **61**, 14095 (2000). [4] S. Suzuki *et al.*, *JPCC*, **117**, 22123 (2013). [5] D. C. Elias *et al.*, *Science*, **323**, 610 (2009).